Similarities of multiple fracturing on a neutron star and on the Earth

Vladimir G. Kossobokov and Vladimir I. Keilis-Borok
International Institute of Earthquake Prediction Theory and Mathematical Geophysics, Russian Academy of Sciences, 79-2 Warshavskoe Shosse, Moscow, Russia

Baolian Cheng
Los Alamos National Laboratory, Los Alamos, New Mexico 87545
(Received 24 September 1999)

In this paper the similarities of multiple fracturing on a neutron star and on the Earth are explored, including power-law energy distributions, clustering, and the symptoms of transition to a major rupture. These similarities may reflect a scenario of a critical transition, common for a broader class of nonlinear systems.

PACS number(s): 05.40.−a, 05.45.−a, 91.45.−c, 68.35.Rh

Flashes of energy radiated by a neutron star in the form of soft γ-ray repeaters (SGR's) [1,2] are probably generated by starquakes analogous to earthquakes. The source of a starquake is a fracture in the neutron star crust, which may release strain energies up to 10^{46} erg [3]. The recorded SGR1806-20 sequence shows not only the power-law energy distribution [4], but also symptoms of a transition to the main rupture common with earthquake sequences. The subsequent decline of activity in the series of ''aftershocks'' also follows the law founded for earthquakes. Thus the limits of similarity in the dynamics of the multiple fracturing are dramatically expanded.

Starquakes provide the drastic extension of the realm of multiple fracturing previously observed in an already broad variety of conditions, from the lithosphere of the Earth through geotechnical and engineering constructions to laboratory samples of solid materials [5,6]. The energy released by observed fractures ranges from 10^{26} erg for the strongest earthquakes down to a fraction of an erg for laboratory samples. Starquakes occur in an even more different environment of a neutron star. The star 1806-20, whose crust has an average density $\gtrsim 10^{14}$ that of the Earth, period of rotation 7.5 s, and magnetic field of 10^{15} Gauss, produced energy by fracture up to 10^{42} erg in γ rays [4]. The solid crust, where starquakes occur, is about 1 km thick; it is made of a solid lattice of heavy nuclei, with electrons flowing, somewhat like a terrestrial metal but much denser. Large differences in forces load the crust causing fracturing. On the Earth convection currents in the mantle provide these forces. On neutron stars convection ceases about 20 s after they form, so that such forces are unavailable. The crust of a neutron star is loaded instead by super-strong stellar magnetic forces as the field drifts through it.

The discrete cascades of multiple fracturing are believed to be chaotic, so that only after certain averaging the regular properties emerge. These are power-law energy distributions [5–7], clustering in many forms [8–10], and certain symptoms of transition to a major rupture, called in seismology premonitory seismicity patterns [11,12]. (A broader overview of chaos and self-organization in multiple fracturing, with emphasis on earthquakes, is given elsewhere [13–16].) These properties exist in diverse conditions, previously explored. Here, we check whether the similarity of multiple fracturing extends to a neutron star, transcending its fantastic difference.

SGR1806-20 SEQUENCE

The 111 starquakes with celestial coordinates 1806-20 were recorded during continuous observation from August 1978 to April 1985 (Fig. 1). They occurred about 40 000 years ago. The observed energy of an event varies from 1.4×10^{40} erg to 5.3×10^{41} erg. Note that the observed energies of earthquakes are observed in a much wider relative energy range, about 14 units of decimal logarithmic scale. SGR1806-20 is the longest sequence attributed to the same neutron star. No other sequence long enough for our analysis has been identified so far.

ENERGY DISTRIBUTION

A fundamental property of multiple fracturing is the power-law distribution of energy $\log_{10} N(E) = a + b \times \log_{10} E$, known in seismology as the Gutenberg-Richter law [5–7]. Here E is the energy of an event; $N(E)$ is the number of events of energy above E. Typically $b = 2/3$. This is a first approximation valid over a sufficient period and territory for a certain energy range $(E_{\min}, E_{\max})$.

Figure 2(a) shows the energy distribution for SGR1806-20. In spite of the narrow energy range it shows the Gutenberg-Richter law (as the linear part of the graph). Its slope, $b = 1$ is within the limits observed for the earthquakes.

Moreover, as is the case for the earthquakes in many regions, the graph bends down at large energies. Such a bend is inevitable since the maximum energy release is limited by the size of the crust and energy density. On the other hand, in the presence of the largest earthquakes the downward bend may disappear or may even reverse to an upward bend. One may speculate that larger starquakes are possible on 1806-20.

Figure 2(b) shows the energy distribution separately for starquakes before the main event on November 16, 1983, $E = 5.17 \times 10^{41}$ erg and after it. We see that the Gutenberg-Richter law holds in each case: the distributions are close to linear on a considerable part of the energy range. However, contrary to what is observed on earthquakes [9] after the largest event is smaller than before it.

CLUSTERING

Earthquakes tend to occur in time-space clusters [8–10]. The most prominent among these are *foreshocks–main*

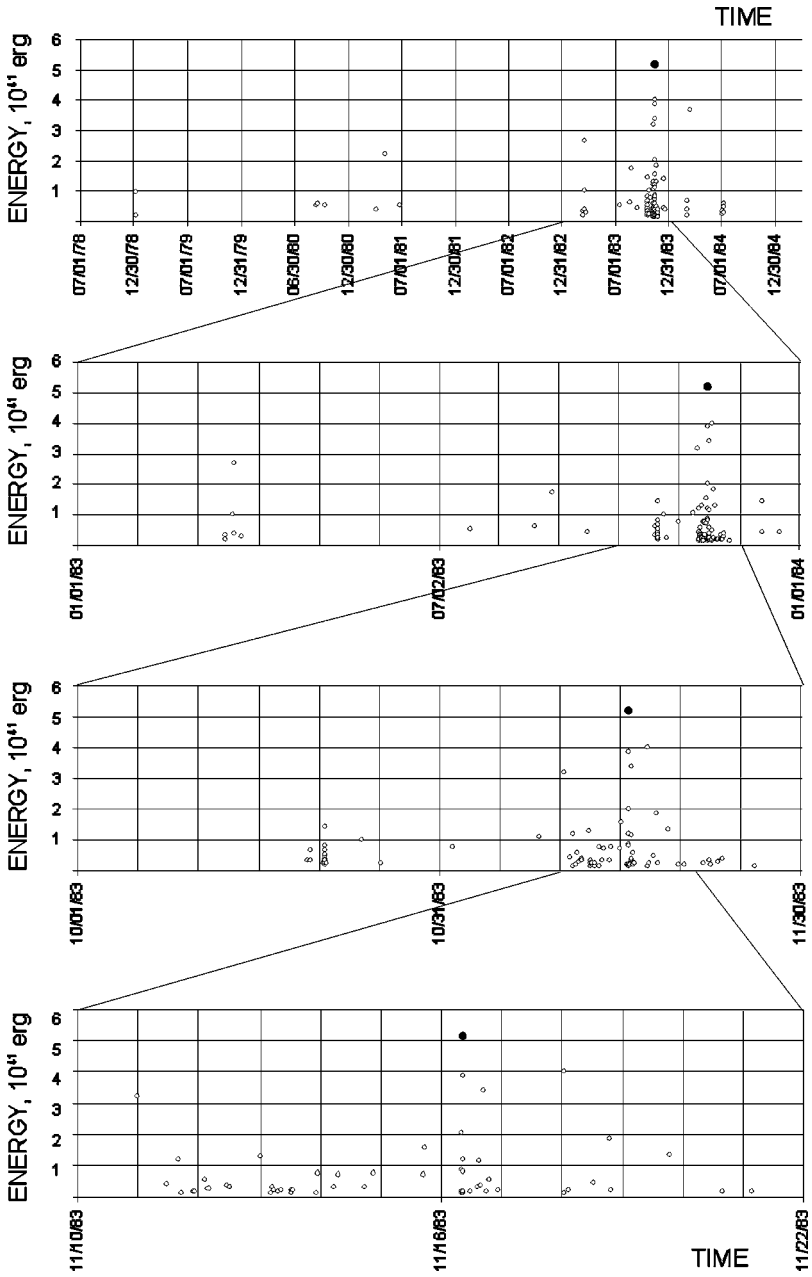

FIG. 1. The SGR 1806-20 sequence of starquakes [1,2]. Time refers to registration; starquakes occurred at the distance of about 40 000 light years. The largest event, November 16, 1983, 8:34 GMT, $E=5.17\times10^{41}$ erg, is marked as a solid dot.

shock–aftershocks sequences and *swarms* of earthquakes. The main shock is the largest earthquake in a sequence, foreshocks are rather rare, and aftershocks are usually numerous. The rate of aftershocks occurrence decreases with time following the Omori law: $\lambda(t)=t^{-(1+\alpha)}$, where $\lambda(t)$ is the intensity of the aftershock activity at time t after the mainshock. The members of a swarm have about the same energy.

The association of starquakes into clusters is rather clear from Figs. 1 and 3. We see a number of clusters before the main event. Half of the starquakes that precede the main event happen in the last seven days, in the last 30 min five ''foreshocks'' occurred. The main event has a prominent sequence of ''aftershocks.'' The first happened one second after [not shown on Fig. 3(b)], the first five happened in 200 min. The Omori law (with $\alpha=0.18$) can be seen as a linear segment of the graph in bilogarithmic scale between 200 min and 100 days.

SYMPTOMS OF TRANSITION TO THE MAIN RUPTURE

This is a rich property of multiple fracturing [11,12] that comprises the energy distribution and clustering, although it is not as well established yet as the other two properties. As already mentioned, Figs. 1 and 3 demonstrate an escalation of fracturing lasting nearly 1000 days and culminated with the largest starquake on November 16. The escalation is expressed both in the intensity of starquake occurrence and in the energy release. The starquakes come more frequency and in larger clusters.

A similar progression is observed in many earthquake sequences, e.g., the one presented in Fig. 4(b). An integral measure of fracturing called the ''cumulative Benioff strain release'' $\varepsilon(t)$ was used to define such progressions [17,18]. It sums up the square root of the energy $E^{1/2}$ for consecutive events. It was suggested [19–21] that a power-law rise of

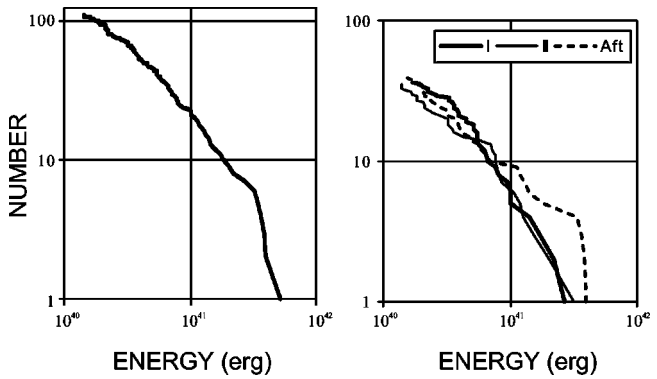

FIG. 2. Cumulative energy distribution of starquakes in SGR 1806-20. The linear segment of the graph suggests the analog of the Gutenberg-Richter law for all 111 starquakes (right), as well as for starquakes before the main event and for its ''aftershocks'' (left: I—first 35 events; II—next 35 events; Aft—the main and subsequent events).

$\varepsilon(t)$ culminates with the largest earthquake, and is accompanied by logarithmic-periodic variations of $\varepsilon(t)$. Specifically, $\varepsilon(t)=A-Bt^m\{1+C\cos(\omega \ln t)\}$, where t is the time to the largest earthquake. Figure 3 shows the power-law increase of $\varepsilon(t)$ for SGR 1806-20 as a linear segment of the graph in a bilogarithmic scale. Moreover, one can observe a possible trace of four logarithmic-periodic oscillations.

Let us check now whether or not the main starquake of November 16 is preceded by other premonitory patterns of seismicity tested worldwide [22–26]. They are detected in the background seismicity, ''a static state,'' which consists of the earthquakes smaller than the earthquakes, targeted for prediction. The progression of starquakes to the main event (Figs. 1 and 3) fits the qualitative description of the intermediate-term premonitory patterns [25,26] with a lead time of the order of years: ''*Before a strong earthquake the earthquake flow in a medium magnitude range becomes more intense and irregular, earthquakes become more clustered in space and time....*''

Algorithms for unambiguous reproducible determination of premonitory patterns can be schematically described as follows. We compute in the running time-windows certain robust characteristics of the ''static state'' within an area considered. When the characteristics become anomalous we detect a premonitory pattern. The patterns are used either alone or in a combination. Their definition is normalized, so that they can be applied without additional adaptation in different energy ranges.

Figure 4(a) shows five premonitory patterns detected by such algorithms before the largest starquake.

(i) Pattern Σ is the large value of the sum of the areas S ruptured in the earthquakes' sources [22]. The coarse estimate $S\sim E^{2/3}$ is used.

(ii) Pattern B is the large number of aftershocks after some mainshock [23].

(iii) Characteristics used in prediction algorithm M8 [24]. Besides B, they include large values of the number of events N, its deviation from long-term trend L and the linear concentration of sources Z.

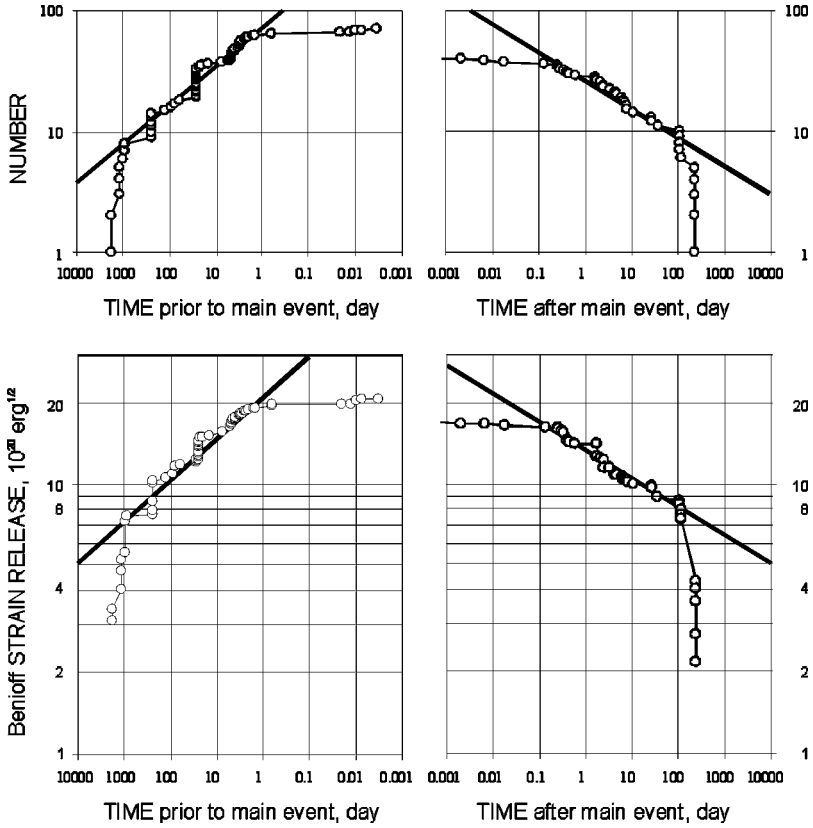

FIG. 3. Progression of starquakes: The cumulative numbers of events preceding (left) and following (right) the main event on November 16 are given at the top. Note that the accumulation of starquakes after the main event is made in reverse time (i.e., from April 1985 to the time of the main event on November 16). Straight lines highlight the nearly linear parts of the graphs that correspond to power-law rise and decay, correspondingly. At the bottom similar graphs for the cumulative ''Benioff strain release'' are given.

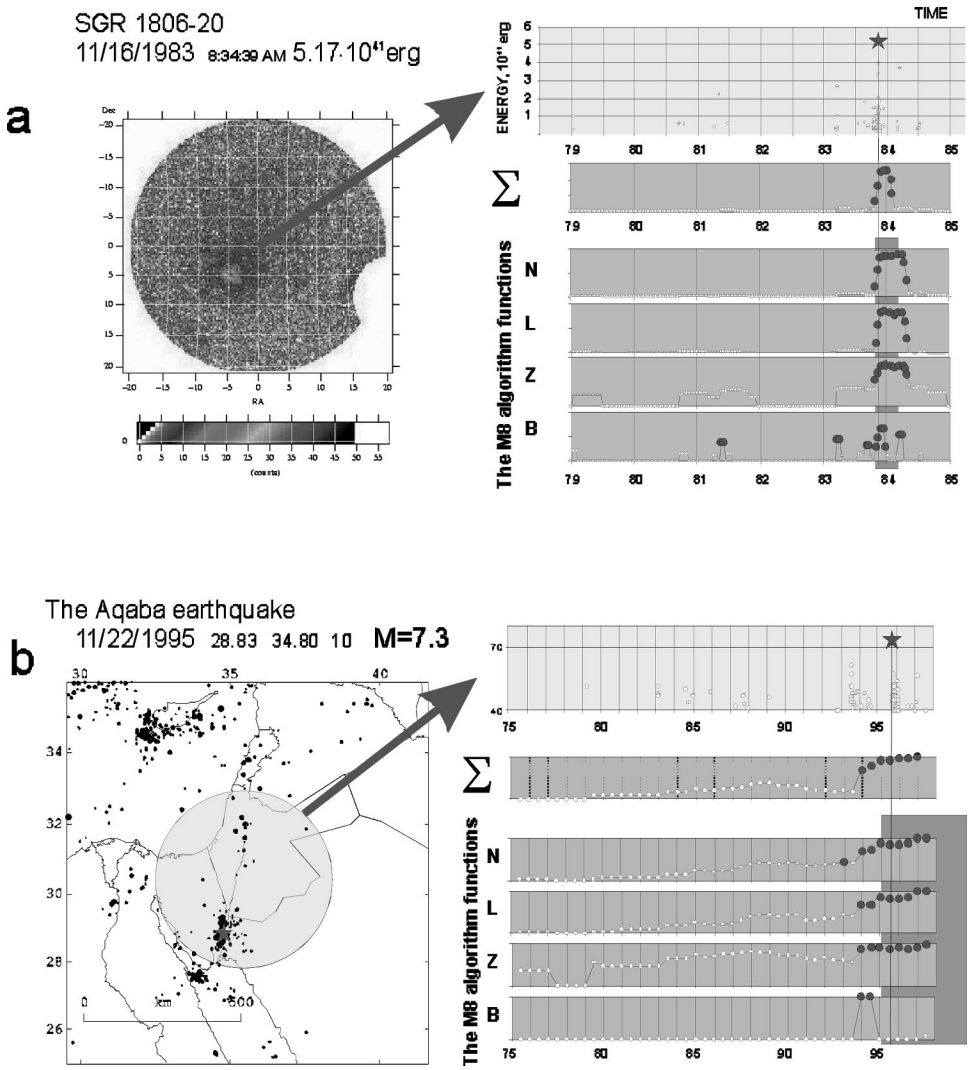

FIG. 4. Premonitory patterns before the main starquake on November 16, 1983 (a) and before the Aqaba earthquake on November 22, 1995 (b). The location is presented at the top. The ''static state'' is plotted with the main event marked by a star. Beneath, the graphs of integral measures of the ''static state'' are given. Their anomalous values are highlighted by enlarged solid dots. Note that the anomalous values precede the main event in both cases. For the M8 algorithm, we outline also the alarm (shaded rectangle). The patterns Σ, N, L, and B are measured, respectively, in $\mathrm{erg}^{2/3}$ per unit time, number per unit time, number per unit time squared, and number. Z is the dimensionless linear concentration.

As one can observe in Fig. 4(a), the patterns closely precede the largest starquake. For comparison with earthquakes, we show a similar result [27] for the sequence preceding the 1995 Aqaba earthquake [Fig. 4(b)]. The patterns are premonitory for both sequences.

Table I illustrates the validity of the premonitory patterns of seismicity. It summarizes the results of advance prediction by the algorithm M8 [28]; the last seven largest earthquakes of the world, $M \geqslant 8$, were predicted justifying a high statistical significance level of the method.

It should be emphasized that the similarity of premonitory patterns for starquakes and earthquakes is only qualitatively established so far. One or two numerical parameters of each algorithm had to be readjusted because of the small number of observed starquakes (just 111) and the narrow range of their energy in logarithmic scale (for earthquakes it would be equivalent to a magnitude interval of about one unit). We have also readjusted the time scale for starquakes since their dynamics evolves much faster than the dynamics of earthquakes. This is illustrated by a comparison of the sequences shown at the top of Figs. 4(a) and 4(b). We assume, hypothetically, that six years for starquakes are equivalent to 80 years for earthquakes, as far as a transition to the main event is concerned. For pattern B we used an alternative definition,

TABLE I. Performance of the M8 algorithm aimed at prediction of magnitude 8.0 or greater earthquakes in the Circum Pacific seismic belt [27]. We distinguish two time intervals, the first starts after the algorithm was published and the second one after the algorithm was set up for research testing in a real-time prediction experiment [29].

Test period	Large earthquakes		Space-time occupied by alarms (%)	Significance level (%)
	Predicted	Total		
1985–1997	7	7	33.4	99.86
1992–1997	5	5	31.3	99.40

practically equivalent to the standard one: we counted the events with weight S (the same as in pattern Σ) to compensate for the narrow energy range.

DISCUSSION

Did we find in SGR1806-20 the major properties of earthquake sequences? Yes, but only with readjustments of some numerical parameters in definitions designed for earthquakes. Therefore we have established, in a strict sense, only the qualitative similarity of the properties considered. However, even that seems striking, since for the earthquakes themselves the similarity of premonitory phenomena is broad but not unlimited: Some premonitory patterns of fracturing are common for steel samples, mines, and medium and large earthquakes, while other patterns of the same kind are different for earthquakes in different tectonic regions [29].

The SGR1806-20 sequence has a simple structure—it is a sequence of well-separated escalating clusters. The clusters of starquakes on October 20 and 21 and on November 11–16 have generated all premonitory patterns. Figure 3 shows a consecutive rise of activity at different time scales. This observation suggests that the premonitory patterns can be found at different time scales as well. This may occur in the regions of medium or low seismicity where separate clusters of earthquakes may organize in a similar escalating structure. The Aqaba sequence [Fig. 4(b)] is one of these cases.

If the similarity discussed here really exists, how do we explain it, given the huge difference in conditions on the Earth and the neutron star? The simplest answer is that the multiple fracturing may reflect a critical transition, common for a broader class of nonlinear systems [13,14,30,31].

ACKNOWLEDGMENTS

A large part of this study, was made at the Abdus Salam International Center for Theoretical Physics. The study was supported also by grants from NSF, INTAS, RFBR, and ISTC. The work of B.C. was supported in part by the U.S. Department of Energy.

[1] C. Thompson and R. C. Duncan, Mon. Not. R. Astron. Soc. **275**, 255 (1995).
[2] J. P. Norris, P. Herz, K. S. Wood, and C. Kouveliotou, Astrophys. J. **366**, 240 (1991).
[3] G. Baym and D. Pines, Ann. Phys. (N.Y.) **66**, 816 (1971); B. Link and R. I. Epstein, Astrophys. J. **457**, 844 (1996).
[4] B. Cheng, R. I. Epstein, R. A. Guyer, and C. Young, Nature (London) **382**, 518 (1995).
[5] G. I. Barenblatt, *Similarity, Selfsimilarity, and Intermediate Asymptotics* (Cambridge University Press, Cambridge, U.K., 1996).
[6] D. L. Turcotte, *Fractals and Chaos in Geophysics*, 2nd ed. (Cambridge University Press, Cambridge, U.K., 1995).
[7] G. Molchan, T. Kronrod, and G. Panza, Bull. Seismol. Soc. Am. **87**, 1220 (1997).
[8] G. Molchan and O. Dmitrieva, Phys. Earth Planet. Inter. **61**, 99 (1990).
[9] G. Molchan and O. Dmitrieva, Geophys. J. Int. **109**, 501 (1992).
[10] Y. Ogata, J. Geophys. Res. **97**, 19 845 (1992).
[11] Earthquake Prediction: The Scientific Challenge. Papers presented at the National Academy of Science Colloquium, Irvine, California, 1996, edited by L. Knopoff [Proc. Natl. Acad. Sci. USA **93**, No. 8 (1996)].
[12] V. I. Keilis-Borok, Physica D **77**, 193 (1994).
[13] D. L. Turcotte, C. A. Stewart, and J. Huang, in *Chaotic Processes in the Geological Sciences*, edited by D. A. Yuen, (Springer-Verlag, New York, 1992), pp. 89–109.
[14] *Nonlinear Dynamics and Predictability of Geophysical Phenomena*, edited by W. I. Newman, A. Gabrielov, and D. L. Turcotte, Geophysical Monograph Series (IUGG-AGU, Washington, DC., 1994).
[15] *SFI Studies in the Science of Complexity*, edited by J. Rundle, D. Turcotte, and W. Klein (Addison-Welsey, Reading, MA, 1996), Vol. XXV.
[16] Dynamics of Lithosphere and Earthquake Prediction. Papers presented at the Fourth International Workshop on Nonlinear Dynamics and Earthquake Prediction, Trieste, Italy, 1997, edited by V. I. Keilis-Borok and P. N. Shebalin [Phys., Earth Planet. Inter. **111**, No. 3–4 (1999)].
[17] D. J. Varnes, Pure Appl. Geophys. **130**, 661 (1989).
[18] C. G. Bufe, S. P. Nishenko, and D. J. Varnes, Pure Appl. Geophys. **142**, 83 (1994).
[19] D. Sornette and C. G. Sammis, J. Phys. I **5**, 607 (1995).
[20] W. I. Newman, A. Gabrielov, and D. L. Turcotte, Phys. Rev. E **52**, 4827 (1995).
[21] C. G. Sammis, D. Sornette, and H. Saleur, in *SFI Studies in the Science of Complexity*, edited by J. Rundle, D. Turcotte, and W. Klein (Addison-Welsey, Reading, MA, 1996), Vol. XXV.
[22] V. I. Keilis-Borok and L. N. Malinovskaya, J. Geophys. Res. **69**, 3019 (1964).
[23] V. I. Keilis-Borok, L. Knopoff, and I. M. Rotwain, Nature (London) **283**, 259 (1980).
[24] V. I. Keilis-Borok and V. G. Kossobokov, Phys. Earth Planet. Inter. **61**, 57 (1990).
[25] V. I. Keilis-Borok, Proc. Natl. Acad. Sci. USA **93**, 3748 (1996).
[26] V. G. Kossobokov, L. L. Romashkova, V. I. Keilis-Borok, and J. H. Healy, Phys. Earth Planet. Inter. **111**, 187 (1999).
[27] V. G. Kossobokov and L. L. Romashkova, in Proceedings of the XXVI General Assembly European Seismological Commission, Tel Aviv, Israel, 1998 (unpublished).
[28] J. H. Healy, V. G. Kossobokov, and J. W. Dewey, U. S. Geol. Surv. OFR 92-401 (1992).
[29] I. V. Rotwain and L. Botvina, Phys. Earth Planet. Inter. **101**, 61 (1997).
[30] B. E. Shaw, J. M. Carlson, and J. S. Langer, J. Geophys. Res. **97**, 479 (1992).
[31] S. L. Pepke, J. R. Carlson, and B. E. Shaw, J. Geophys. Res. **99**, 6769 (1994).